

Tuning the Transdermal Transport by Application of External Continuous Electric Field: A Molecular Dynamics Coarse-Grained Study

Neila Machado¹, Clarissa Callegaro², Marcelo Augusto Christoffolete¹, and Herculano Martinho*

¹Centro de Ciências Naturais e Humanas, Universidade Federal do ABC, Av. dos Estados 5001, Santo André-SP, 09210-580, Brazil

²AXCEM Dermatologia, Cosmiatria e Laser, R. Távares Cabral, 102, conj. 71, São Paulo-SP, 05423-030, Brazil

Abstract

Since a long time the application of small electric potentials on biological membranes (iontophoresis) proved enabling control and improvement of transdermal delivery of substances across this barrier. In spite of a large experimental data, the detailed molecular mechanism of iontophoresis is absent. In the present work the interaction among the external continuous electric field with the outermost layer of the skin (*stratum corneum*) was studied by coarse-grained molecular dynamics. Our results pointed out the occurrence of water-rich vesicles formation depending on the field strength. The corresponding phase diagram indicated that the large set of phenomena (vesicle formation, reversibility, phase transition, disruption) could be completely controlled by tuning external continuous electric fields. Interestingly, electric field shielding effects are in the origin of observed effects and followed a general Arrhenius-like time dependence. Direct current (DC) electric field usage would also have booster diffusion effects due to vesicles creation and reincorporation which would have direct beneficial absorption effects on water-soluble topical agents (vitamins) or dermal jet-injection of drugs by fine needles.

Keywords: stratum corneum; skin; molecular dynamics; tissue computer model; electroporation; iontophoresis.

1. Introduction

The human skin is a natural barrier to the transport of substances. Skin controls the detailed balance of, e.g., moisture and harmful molecules. It protects the body against external chemical and physical factors, takes part in the metabolic processes, plays a resorptive and thermoregulatory function, and it partakes in immunological processes[1, 2]. In fact, it is a complex organ that has many functions that go far beyond its role as a barrier to the environment[1].

The basic structure of the skin comprises three component layers: epidermis, dermis, and hypodermis[3]. The epidermis is the outer layer of the three layers that make up the skin[3]. It is divided into four layers, starting at the dermal junction with the basal cell layer and ending at the outer surface in the *stratum corneum* (SC) membrane[4]. SC is the main responsible for the selective permeability of exogenous substances. The SC is organized in an arrangement known as "bricks and mortar" where the keratinized cells called corneocytes represent the "bricks" and are embedded into a highly specialized intercellular cement known as the extracellular matrix or lipid matrix[5]. This structured bilayered matrix is mainly composed by ceramide, cholesterol, and free fatty acids molecules. The detailed composition and amount of bilayers vary as function of the depth of the SC[1, 3, 4, 6]. This multilamellar

system is responsible for the maintenance and homeostatic balance of the skin[1, 3, 4, 6].

The SC is a rate-limiting lipophilic barrier against the uptake of chemical and biological toxins, as well as trans-epidermal water loss[7, 8]. Several approaches have been proposed to control the permeability of this barrier (see, e.g., [9] and [10]). Such control would enable to establish viable and advantageous optional routes for the administration of medications, vitamins, and nutrients[11]. The transdermal delivery could for example, reduce first-pass metabolism associated with oral delivery, and is not painful as injections[12].

A number of factors affects the dermal absorption, including, e.g., type of skin; physical-chemical properties of delivery systems; skin moisture level; external temperature; skin pre-treatment; among others. Thus, numerous *in-vitro* and *in-vivo* models are used to examine the penetration of active compounds through the skin[8, 13]. Notwithstanding, several issues such as permeability and dermal absorption processes, remain unsolved.

The application of external electric fields in the biological membranes aiming enable the transport of substances across this barrier is known as *electroporation*. The effect can be either reversible or irreversible[14, 15]. The reversible electroporation has become an important tool in biotechnology and medicine. There are several reports considering the fusion of cells, treatment of cancer, and transdermal delivery of drugs and genes using reversible electroporation (see, e.g., [15]). Irreversible electropora-

*Corresponding author: herculano.martinho@ufabc.edu.br

tion also have is also an important medical technology as, e.g., tissue ablation tool for treatment of elusive cancers such as in the prostate, the lung and the brain[16].

Furthermore, electroporation is widely used as a delivery method for small DNA transfection in cell culture as well *in vivo*[17]. It is also used to transform bacteria as standard procedure in molecular biology. It is reported to present superior efficiency compared to chemical or thermal shock techniques[17]. Therefore, efficiency improvement in electroporation protocols is very desirable.

The electric field pulses usually employed experimentally have intensities of ~ 1 mV/nm and exposure duration of few milliseconds[15]. The temporary pores formed are difficult to be directly observed since their dimensions (several nanometers) and instability fall out the limits of current electron microscopy soft matter experimental techniques[15]. Thus, the concretely established characteristic of the electroporation include the creation of a transient charge state where there is a rapid and reversible increase in permeability, electrical conductance and a decrease in membrane resistance[14, 15].

In-silico approaches are in principle able to predict adsorption, distribution, metabolism, excretion, and toxicity on the basis of input data describing physical-chemical properties of the compounds to be delivered and on physiological properties of the exposed skin[18–25]. In particular, classical molecular dynamics have been used to perform permeability studies at molecular level[22–25].

The change caused by pulsed electric fields on the lateral organization of cell membranes is widely reported on literature (see, e.g.,[25–27]). The first work reporting a possible molecular mechanism for pore formation in the skin lipid bilayer during electroporation was the molecular dynamics simulation by Gupta and Rai[25]. They studied the effect of the applied external electrical field (0.6 – 1.0 V/nm) on the pore formation dynamics in the lipid bilayer of different sizes (154, 616, and 2464 lipids) and compositions (ceramide/cholesterol/free fatty acid, 1:0:0, 1:0:1, 1:1:0, 1:1:1). They reported that the electroporation process was found to be reversible for the setted parameters. The authors also reported that the pore-opening dynamics depends upon the strength of the applied electric field, whereas the pore-closing dynamics is independent of the applied electric field. The interfacial water played a key role in the electroporation of the skin lipid bilayer.

The external disturbances can lead to membrane reorganization at different levels, e.g., affecting organizational tendencies such as compartmentalization and groupings[26]. In membranes with different amounts of cholesterol molecules in their composition, the application of electric fields leads to the formation of pores with different morphologies, when compared to the hydrophilic pores often formed in phospholipid membranes[28–30]. These morphological differences have impact on the transport properties of such electroporated membranes.

The simulation studies by Casciola *et al.*[30] concluded that electroporation of cholesterol-rich membranes is strongly

influenced by this compound in agreement with previous studies of Koronkiewicz and Kalinowski [29]. The former authors shown that the pores formed in membranes containing cholesterol close during electroporation and non-stabilized pores of the phospholipid head groups collapse and seal much more rapidly.

In the molecular dynamics studies investigating the thermodynamic effect on dipalmitoylphosphatidylcholine (DPPC) bilayers with different cholesterol concentrations, Bennet *et al.*[31] reported that cholesterol was able to increase the order, thickness and stiffness of these bilayers, restricting deformations of the bilayer and preventing the formation of pores. They suggested that large thermal fluctuations are involved in the budding and fusion of vesicles, in the passive lipid flip-flop and pore formation. The increased concentration of this molecule promoted the increase of the free energy barrier to transfer the sets of DPPC heads to the center of the bilayer by lowering the velocity of the DPPC flip-flop in orders of magnitude.

Fernández *et al.*[32] calculated the electroporation field threshold on DOPC bilayers with different cholesterol concentrations. They reported that membranes containing cholesterol presented greater electric field threshold for electroporation, slower kinetics, and higher cohesion as well.

The application of continuous small electric potentials enables control and improvement of transdermal molecules delivery[33, 34]. This methodology is named iontophoresis and has medical applications for treatment and diagnosis in a broad range of pathologies as hyperhidrosis[35], ophthalmology[34], cystic fibrosis[36], anaesthesia[37], cancer [38], among others (see, e.g.,[39]). The typical electrical currents can vary between 0.5 and 30 mA/cm² which is applied for minutes or hours[40–42]. The technique enables transdermal administration and provides programmable drugs dosage by setting the electric current. It helps to make drug absorption less dependent on biological variables[41]. In spite of their relevance, to the best of our knowledge there are a lack of computational simulations studies concerning the molecular mechanisms of iontophoresis and electroporation as well. Its exact action mechanisms still obscure[43]. Moreover, in order to have a complete picture about the action of external electric fields over biological membranes, the low intensity, continuous field is an important limit case to be studied. In this work the interaction of low intensity static electric fields and SC model of human skin was studied using molecular dynamics (MD).

2. Methodology

In this study, MD was used in the coarse-grained (CG) approach[44–46]. This methodology allows the simulation of large and complex systems such as biological ones, providing a complete description that is beyond the dimensions usually explored in the actual soft matter experimental studies. All simulations were implemented in the GROMACS MD v.2018.1[47–49].

The SC model was developed and describe elsewhere by one of the authors[23]. It uses the composition of the lipid matrix region (lamellar region between the corneocytes): i) ceramide type II (24%), which forms a dense bilayer and acts on the input control of water molecules making the membrane less permeable compared to the membrane of phospholipids; ii) cholesterol(36%), which acts as a molecular "clamp" between the larger molecules and which is also involved in membrane fluidity; iii) fatty acid (tetrasanoic acid, 39%) which decreases the packaging of the membrane (Fig. 1a). The polarized water is explicitly included in this SC model[50]. The membrane was modeled using the INSANE[51] program and contained 65,166 polarized water beads. Na^+ and Cl^- ions were incorporated into the system. Thus, the initial system totaled 69,462 molecules. The total volume of the simulation was defined in a box of $25 \times 25 \times 18 \text{ nm}^3$.

We used the Martini force-field[44, 45]. For integration of Newton's equations of motion it was used the leap-frog algorithm[52] in order to obtain the MD trajectories. The integration time step was 20 fs. The search for the neighborhood was using the Verlet scheme[53]. For the treatment of Coulomb forces we use the reaction-field/potential-shift with a cutting radius of 1.1 nm. For the van der Waals interactions we used the cut-off/potential-shift with Lennard-Jones cutoff radius of 1.1 nm. The dielectric constant was set to 15 which is a value very close to the dielectric constant of membrane lipids [54, 55]. For temperature control we used the V-rescale thermostat (a modified Berendsen type)[56, 57]. A temperature bath of 310 K was chosen due to its approximate value to the human physiological temperature. In order to control the pressure, the Parrinello-Rahman[58] barostat was used to couple the system to semi-isotropic pressure of 1 atm with compressibility of 3×10^{-4} bar along the x- and y-axis directions. The axis between the bilayers was chosen along x-direction (see Fig.1a). Periodic boundary conditions were applied in the directions of the x, y, and z axes.

The constant electric field was applied along the z-axis (E_z) using the GROMACS implementation by Caleman and Spoel[59]. We notice that the induced electric field from the dipoles on the simulation box (E_{dp}) was always $E_{dp} \sim 10^{-10} E_z$. Thus, the effects of E_{dp} could be neglected. The temporal evolution in each situation was monitored, looking for frequent structural alterations. Before application of the electric field, the system was relaxed by running 1000 ns of trajectory simulation. The minimized state resulted in a set box at $18.63 \times 18.63 \times 29.76 \text{ nm}^3$. It was used as the basis for the subsequent simulations and variations of electric field intensities. The results where visualized using the VMD program[60].

3. Results and discussion

We analyzed the effects of electric field in the range $E_z = 0 - 100 \text{ mV/nm}$. The results are presented and

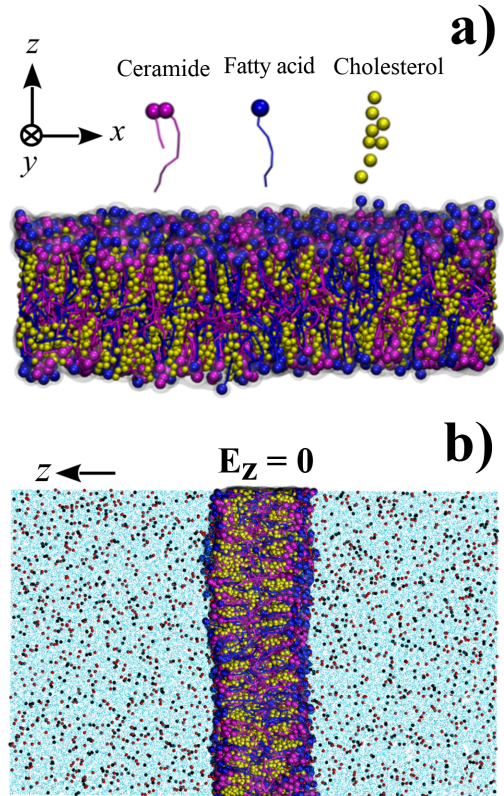


Figure 1: **a)** Coarse-grained representation for the human *stratum corneum* lamellar lipidic membrane containing ceramide (24%), fatty acid (39%), and cholesterol(36%). The membrane thickness is 5.4 nm. The depth of the bilayer was oriented along z-axis following the oriented axis set shown in the inset. **b)** Initial state of the simulation box in the zero-field condition. The dimensions of box are $25 \times 25 \times 18 \text{ nm}^3$. The membrane is surrounded by water (cyan) and ions (Na^+ , red dots and Cl^- , black dots)

discussed on the following. A summary of findings is presented on Table 1.

Table 1: Summary of findings in the vesicle dynamics as function of electric field strength.

E_z (mV/nm)	Total time (ns)	Qualitative Description
≤ 6	1000	absence of effects
7; 8	1000	waviness deformation in the membrane; water incorporation in the core; reversible iontophoresis
9	1000	ripping off vesicle with water in the core; irreversible iontophoresis
10	1000	ripping off vesicle with water in the core; membrane unstable after vesicle re-incorporation; irreversible iontophoresis
20 – 100	1 – 100	fragmentation of the membrane; irreversible iontophoresis

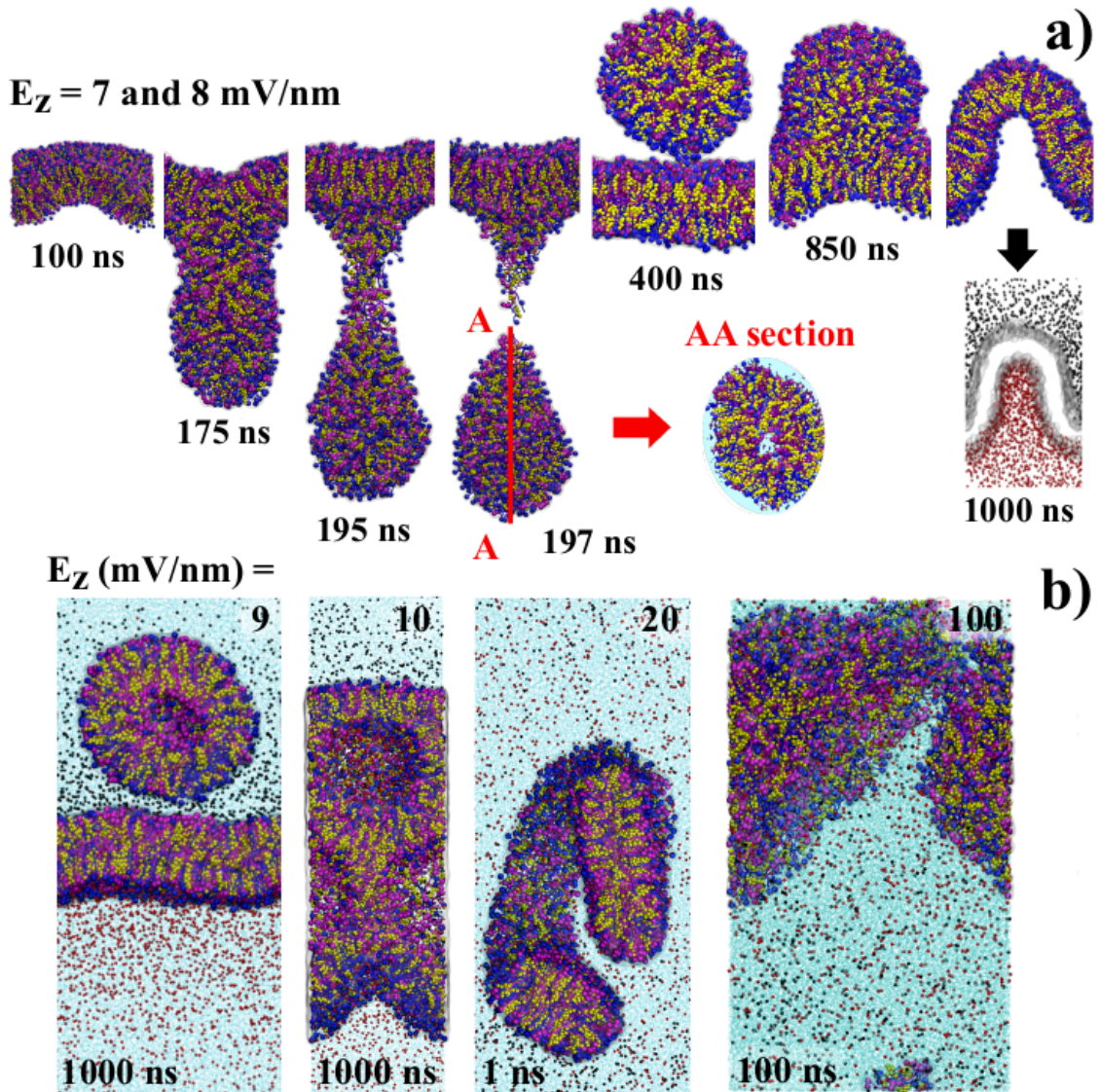


Figure 2: **a)** Temporal evolution up to 1000 ns for z-axis applied electric fields $E_z = 7$ and 8 mV/nm. For these intensities the detachment/attachment of a vesicle was observed. The vesicle encapsulates water molecules in the core and also in an internal shell close to the surface as shown in the AA section of 197 ns snapshot. The detachment was completed at this time. At 400 ns the vesicle starts to be reincorporated. At 1000 ns it was completely reabsorbed on the membrane. However, a charge separation was markedly observed as indicated by the bottom frame for 1000 ns. For these field intensities it was observed a reversible iontophoresis. **b)** Final simulation snapshots for $E_z = 9, 10, 20$ and 100 mV/nm. For 9 mV/nm electric field intensity it was observed the detachment of a vesicle which will not return to the membrane. For $E_z = 10$ mV/nm, a vesicle is expelled and returns to the membrane. However the final topology is unstable having a honeycomb pattern (phase transition). The process is irreversible. For 20 mV/nm and 100 mV/nm field intensities the membrane is deformed in different fragments also in a irreversible way.

3.1. Field strength $E_z \leq 6$ mV/nm

Our findings indicate absence of noticeable topological effects on the membrane in this case. Electric fields of this range of intensity only promoted the separation of ionic charges. Zero-field simulations (Fig. 1b) showed a homogeneous ions distribution in the solvent. It was observed that the membrane became more compact (reduction of 20 % in the box volume) as widely reported for membranes with cholesterol in the structure[29].

Structural variations were also absent. In fact, only a slight bending promoted by the proximity of the ions

that were rearranged where observed. Na^+ cations concentrated on the top of membrane (z-axis), and the Cl^- anions on the bottom. The simulation extended beyond $1 \mu\text{s}$ without noticeable changes (see supplementary material).

3.2. Field strength $E_z = 7$ and 8 mV/nm

Applying intensities of 7 and 8 mV/nm field we obtained very outstanding results. The starting deformation in the membrane (see 100 ns snapshot in Fig. 2a) resulted in the later formation of vesicle. This vesicle encapsulated

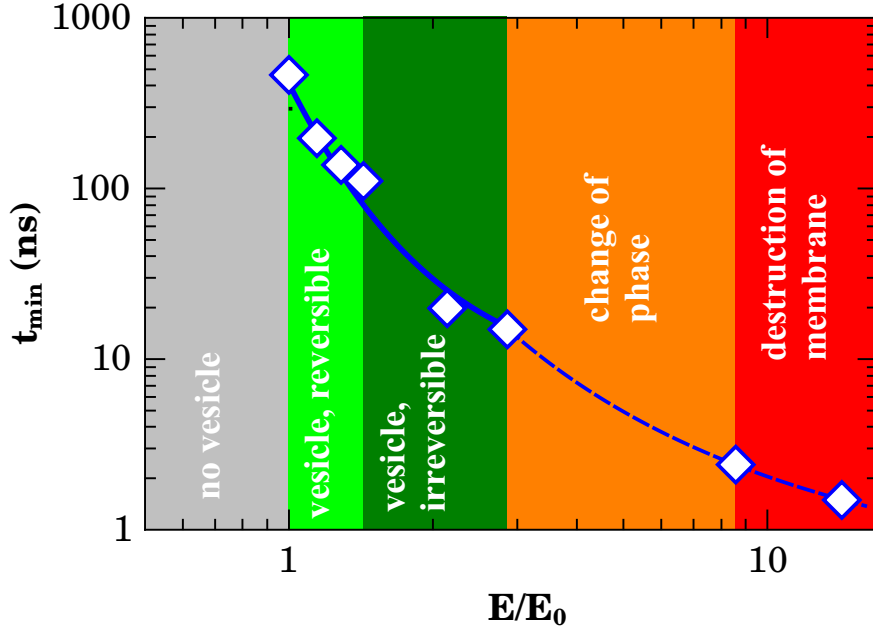


Figure 3: Diagram showing the minimal time for events for *stratum corneum* membrane model (t_{min}) as function of the normalized static electric field strength (E/E_0). The normalizing factor is the minimal electric field where vesicles formation takes place in the simulation ($E_0 = 7$ mV/nm in the present case). The solid and dashed lines are fittings to eq. (1) as described in the text.

water molecules in the core and in an internal shell close to the surface (see AA section of 197 ns snapshot). The detachment was completed at this time. At 400 ns the vesicle starts to be re-incorporated. At 1000 ns it was completely reabsorbed on the membrane. However, a charge separation was markedly observed as indicated by the bottom frame for 1000 ns. For these field intensities it was observed a reversible iontophoresis process.

It was also observed that the vesicle detachment/return occurred $\sim 50\%$ faster for $E_z = 8$ mV/nm. Extending the simulations in both intensities up to 2000 ns, we observed that the process of formation, detachment and re-absorption of the vesicles.

3.3. Field strength $9 \leq E_z \leq 100$ mV/nm

The $E_z = 9$ mV/nm (Fig. 2b) presented similar results of 7 and 8 mV/nm. Notwithstanding the resemblance, the formed vesicle did not return to the membrane. For $E_z = 10$ mV/nm (Fig. 2b) vesicle enclosing water molecules was also formed but the membrane was unable to recover. The vesicle returned to the membrane, but the membrane did not stabilize. The final topology was unstable having a honeycomb pattern. Increasing field strength to 20–100 mV/nm (Fig 2b) resulted fragmentation of the SC membrane leading drastic and irreversible morphological changes. More figures and details considering another fields are available in the supplementary materials section.

The simulations reported on literature are usually based on membranes formed essentially of few kinds of phospholipids subjected to pulsed electric fields of various magnitudes. In general, the reported result is the formation of

hydrophilic pores which are stabilized by the head groups of the phospholipids[14–16, 28–31].

Our results shows the possibility of controlling both water transport across SC and vesicle formation dynamics without large scale membrane compromising by tuning the electric field intensity. In order to summarize the data and give a global phenomenological explanation to the overall picture of the previous results we present the diagram of Fig. 3. In this diagram, the minimal time for relevant events (reversible or irreversible vesicle formation, change of phase or membrane disruption) was plotted against the applied field normalized to the minimal time for events starting ($E_0 = 7$ mV/nm in the present case) in a log-reciprocal scale. The normalization helps to future comparison to experimental data. The data was fitted to an Arrhenius-like dependence

$$t_{min} \propto e^{\frac{\alpha E}{E_0}} \quad (1)$$

Due to the both internal and external charge separation to the vesicles and dielectric constant mismatch as well, the external field is shielded and the local field is decreased in relation to external one. One rough approximation to the effective local field is $E_\alpha = E_0/\alpha$ being α the shielding factor. The solid line shown on Fig.3 presents the best fitting to eq. 1 for data in the vesicle formation region of the diagram ($1 \leq E/E_0 \leq 1.9$). The accordance was excellent for $\alpha = 5.7 \pm 0.3$. In this case, $E_\alpha = 0.175 \times E_0 = 1.2$ mV/nm. For increasing fields strengths where change of phase or destruction of membrane takes place ($E/E_0 \gtrsim 1.9$) the slope of the curve presented a slight change. The best fit (dashed line on Fig. 3) was obtained for $\alpha = 6.7 \pm 0.5$

which furnished $E_\alpha = 0.149 \times E_0 = 1.0$ mV/nm. For comparison effects, the electric field shielding due to the presence of a dielectric sphere is $\alpha \sim 5.3$ [61] which is very similar to our results. Despite the broad values of intensities of applied fields a large diversity of membrane events in the diagram appeared to emerge from the same local field $E_\alpha \sim 1.1$ mV/nm. At first glance, one possible explanation could reside on a viscosity field dependence which would be critical at micro-scale where non-Newtonian phenomena arises[62].

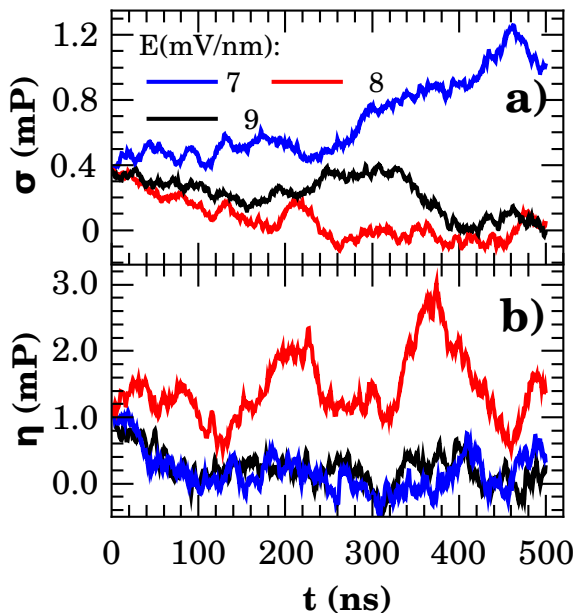


Figure 4: Shear (a) and bulk (b) viscosity of the system under electric field application of 7 (blue), 8 (red), and 9 (black) mV/nm.

Figure 4 presents the shear (σ) and bulk (η) viscosity for 7, 8, and 9 mV/nm applied field intensities. These values delineates the emergence of the main effects observed on phase diagram of Fig.3. The field-dependence of viscosities is remarkable. However, it was not found a clear correlation to the phenomena reported elsewhere. In fact, a more careful analysis of the system dynamics need to be conducted to clarify this point. This important task is beyond the scope of the present work.

4. Conclusions

Despite the well known effects of iontophoresis, its mechanism of work is still poorly understood. Our results indicate that hydration effects related to vesicle formation could be tuned by constant external electrical fields. Our findings indicates that this is the underlying mechanism of iontophoresis. This technique usually employs constant or alternating (5 – 10 kHz) currents [35] for therapeutic purposes. However, we argue that DC field usage would also have booster diffusion effects due to vesicles creation and reincorporation. The application of static electric

field on skin would have direct beneficial absorption effects on water-soluble topical agents as vitamin C[63], vitamin D[64], and vitamin B12[65]. Moreover, the dermal jet-injection of drugs by fine needles[66, 67] could also take advantage from the application of external electric field.

It is the first report of large diversity of phenomena as function of field in the literature, to the best of our knowledge. The phase diagram including reversible/irreversible water-rich vesicle formation, phase transitions, and membrane disruption was presented and would be helpful to experimental verification of our findings. Interestingly, electric field shielding effects are in the origin of observed phenomena following a general Arrhenius-like time dependence. At last, we report that field dependence of both shear and bulk viscosity appeared to play no role in this case.

Acknowledgements. The authors would like to thank the Brazilian agencies Conselho Nacional de Desenvolvimento Científico e Tecnológico (CNPq - 311146/2015-5) and Fundação de Amparo à Pesquisa do Estado de São Paulo (FAPESP - 2011/19924-2) for the financial support. The authors would also thank the computational resources provided by Centro Nacional de Processamento de Alto Desempenho em São Paulo (CENAPAD-UNICAMP) and Sistema de Computação Petaflopica (Tier 0) (Santos Dumont-LNCC) under Sistema Nacional de Processamento de Alto Desempenho (SINAPAD) of the Ministério da Ciência, Tecnologia e Inovação (MCTI).

5. References

References

- [1] Z. Hongbo, H. I. Maibach, *Dermatotoxicology*, 6th edition ed., CRC Press LCC, USA, 2004.
- [2] M. Boer, E. Duchnik, R. Maleszka, M. Marchlewicz, *Structural and biophysical characteristics of human skin in maintaining proper epidermal barrier function*, *Adv. Dermatol. Allergol.* 33 (2016) 1.
- [3] H. G. Burkitt, B. Young, J. W. Heath, *Wheater's functional histology: a text and colour atlas*, 6th ed., Churchill Livingstone, 2014, pp. 159–179.
- [4] J. G. M. J. MD, J. J. M. MD, Lookingbill and Marks' *Principles of Dermatology*, 5e ed., Saunders, 2013.
- [5] C. R. Harding, S. Aho, C. A. Bosko, *Filaggrin - revisited*, *Int. J. Cosmet. Sci.* 35 (2013) 412–423.
- [6] P. M. Elias, *Advances in Lipid Research: Skin Lipids*, *Advances in Lipid Research*, Elsevier Science, 2016. URL: <https://books.google.com.br/books?id=rTeaBQAAQBAJ>.
- [7] L. T. Fox, M. Gerber, J. D. Plessis, J. H. Hamman, *Transdermal drug delivery enhancement by compounds of natural origin*, *Molecules* 16 (2011) 10507–10540.
- [8] A. Herman, A. P. Herman, *Essential oils and their constituents as skin penetration enhancer for transdermal drug delivery: a review*, *J. Pharm. Pharmacol.* 67 (2015) 473–485.
- [9] A. Dabrowska, F. Spano, S. Derler, C. Adlhart, N. Spencer, R. Rossi, *The relationship between skin function, barrier properties, and body-dependent factors*, *Skin Res Technol* 24 (2018) 165–174.
- [10] B. Pecoraro, M. Tutone, E. Hoffman, V. Hutter, A. M. Almerico, M. Traynor, *Predicting skin permeability by means*

- of computational approaches: Reliability and caveats in pharmaceutical studies, *J. Chem. Inf. Model.* (2019).
- [11] H. Wosicka, K. Cal, Targeting to the hair follicles: Current status and potential, *J Dermatol Sci* 57 (2017) 83–89.
 - [12] C. M. Schoellhammer, D. Blankschtein, R. Langer, Skin permeabilization for transdermal drug delivery: recent advances and future prospects, *Expert Opin. Drug Deliv.* 11 (2014) 393–407.
 - [13] B. Godin, E. Touitou, Transdermal skin delivery: predictions for humans from in vivo, ex vivo and animal models, *Adv. Drug Delivery Rev.* 59 (2007) 1152–1161.
 - [14] T. Batista Napotnik, D. Miklavčič, In vitro electroporation detection methods – An overview, *Bioelectrochemistry* 120 (2018) 166–182.
 - [15] T. Kotnik, W. Frey, M. Sack, S. H. Meglič, M. Peterka, D. Miklavčič, Electroporation-based applications in biotechnology, *Trends Biotechnol.* 33 (2015) 480–488.
 - [16] B. Rubinsky, Irreversible electroporation in medicine, *Technol. Cancer Res. Treat.* 6 (2007) 255–259.
 - [17] H. Potter, R. Heller, Transfection by electroporation, *Curr Protoc Mol Biol.* 121 (2018) 9–3.
 - [18] H. Baba, J.-i. Takahara, H. Mamitsuka, In silico predictions of human skin permeability using nonlinear quantitative structure–property relationship models, *Pharm. Res.* 32 (2015) 2360–2371.
 - [19] D. Selzer, D. Neumann, H. Neumann, K.-H. Kostka, C.-M. Lehr, U. F. Schaefer, A strategy for in-silico prediction of skin absorption in man, *Eur. J. Pharm. Biopharm.* 95 (2015) 68–76.
 - [20] T. Hatanaka, S. Yoshida, W. R. Kadhum, H. Todo, K. Sugibayashi, In silico estimation of skin concentration following the dermal exposure to chemicals, *Pharm. Res.* 32 (2015) 3965–3974.
 - [21] G. Verheyen, E. Braeken, K. Van Deun, S. Van Miert, Evaluation of in silico tools to predict the skin sensitization potential of chemicals, *SAR QSAR Environ. Res.* 28 (2017) 59–73.
 - [22] S. J. Marrink, V. Corradi, P. C. Souza, H. I. Ingólfsson, D. P. Tieleman, M. S. Sansom, Computational modeling of realistic cell membranes, *Chem. Rev.* (2019).
 - [23] N. C. F. Machado, L. Dos Santos, B. G. Carvalho, P. Singh, C. A. Tellez Soto, N. G. Azoia, A. Cavaco-Paulo, A. A. Martin, P. P. Favero, Assessment of penetration of Ascorbyl Tetraisopalmitate into biological membranes by molecular dynamics., *Comput. Biol. Med.* 75 (2016) 151–159.
 - [24] P. Rocco, F. Cilurzo, P. Minghetti, G. Vistoli, A. Pedretti, Molecular dynamics as a tool for in silico screening of skin permeability, *Eur. J. Pharm. Sci.* 106 (2017) 328–335.
 - [25] R. Gupta, B. Rai, Electroporation of skin stratum corneum lipid bilayer and molecular mechanism of drug transport: A molecular dynamics study, *Langmuir* 34 (2018) 5860–5870.
 - [26] J. T. Groves, S. G. Boxer, H. M. McConnell, Lateral Reorganization of Fluid Lipid Membranes in Response to the Electric Field Produced by a Buried Charge, *J. Phys. Chem. B* 104 (2000) 11409–11415.
 - [27] M. Tarek, Atomistic simulations of electroporation of model cell membranes, in: *Transport Across Natural and Modified Biological Membranes and its Implications in Physiology and Therapy*, Springer, 2017, pp. 1–15.
 - [28] A. Polak, M. Tarek, M. Tomšič, J. Valant, N. P. Ulrih, A. Jamnik, P. Kramar, D. Miklavčič, Electroporation of archaeal lipid membranes using MD simulations, *Bioelectrochemistry* 100 (2014) 18–26.
 - [29] S. Koronkiewicz, S. Kalinowski, Influence of cholesterol on electroporation of bilayer lipid membranes: chronopotentiometric studies, *Biochim. Biophys. Acta, Biomembr.* 1661 (2004) 196–203.
 - [30] M. Casciola, D. Bonhenry, M. Liberti, F. Apollonio, M. Tarek, A molecular dynamic study of cholesterol rich lipid membranes: comparison of electroporation protocols, *Bioelectrochemistry* 100 (2014) 11–17.
 - [31] W. F. D. Bennett, J. L. MacCallum, D. P. Tieleman, Thermodynamic Analysis of the Effect of Cholesterol on Dipalmitoylphosphatidylcholine Lipid Membranes, *JACS* 131 (2009) 1972–1978.
 - [32] M. L. Fernández, G. Marshall, F. Sagués, R. Reigada, Structural and Kinetic Molecular Dynamics Study of Electroporation in Cholesterol-Containing Bilayers, *J. Phys. Chem. B* 114 (2010) 6855–6865.
 - [33] M. Singhal, Y. N. Kalia, Iontophoresis and electroporation, in: *Skin Permeation and Disposition of Therapeutic and Cosmeceutical Compounds*, Springer, 2017, pp. 165–182.
 - [34] M. R. Prausnitz, R. Langer, Transdermal drug delivery, *Nat. Biotechnol.* 26 (2008) 1261.
 - [35] C. Gollins, A. Carpenter, C. Steen, H. Bulinski, R. Mahendran, A retrospective analysis of the use of tap water iontophoresis for focal hyperhidrosis at a district general hospital: The patients’ perspective, *J Dermatolog Treat.* (2019) 1–9.
 - [36] C. Wallis, Diagnosis and presentation of cystic fibrosis, in: *Kendig’s Disorders of the Respiratory Tract in Children (Ninth Edition)*, Elsevier, 2019, pp. 769–776.
 - [37] F. Liu, L. Liu, Iontophoretic delivery of lignocaine in healthy volunteers: effect of concentration of epinephrine on local anesthesia, *Biomed Res India* 28 (2017) 185–191.
 - [38] J. D. Byrne, J. J. Yeh, J. M. DeSimone, Use of iontophoresis for the treatment of cancer, *J. Controlled Release* (2018).
 - [39] T. Gratieri, Y. N. Kalia, Iontophoresis: Basic principles, in: *Percutaneous Penetration Enhancers Physical Methods in Penetration Enhancement*, Springer, 2017, pp. 61–65.
 - [40] D. G. Kassar, A. M. Lynch, M. J. Stiller, Physical enhancement of dermatologic drug delivery: iontophoresis and phonophoresis, *J Am Acad Dermatol* 34 (1996) 657–666.
 - [41] A. K. Banga, S. Bose, T. K. Ghosh, Iontophoresis and electroporation: comparisons and contrasts, *Int. J. Pharm.* 179 (1999) 1–19.
 - [42] A. Jadoul, J. Bouwstra, V. Preat, Effects of iontophoresis and electroporation on the stratum corneum: review of the biophysical studies, *Adv. Drug Delivery Rev.* 35 (1999) 89–105.
 - [43] M. P. Stewart, R. Langer, K. F. Jensen, Intracellular delivery by membrane disruption: mechanisms, strategies, and concepts, *Chemical reviews* 118 (2018) 7409–7531.
 - [44] S. J. Marrink, A. H. de Vries, A. E. Mark, Coarse Grained Model for Semiquantitative Lipid Simulations, *J. Phys. Chem. B* 108 (2004) 750–760.
 - [45] S. J. Marrink, H. J. Risselada, S. Yefimov, D. P. Tieleman, A. H. de Vries, The MARTINI Force Field: Coarse Grained Model for Biomolecular Simulations, *J. Phys. Chem. B* 111 (2007) 7812–7824.
 - [46] H. I. Ingólfsson, C. A. Lopez, J. J. Uusitalo, D. H. de Jong, S. M. Gopal, X. Periole, S. J. Marrink, The power of coarse graining in biomolecular simulations., *Wiley Interdiscip. Rev.: Comput. Mol. Sci.* 4 (2014) 225–248.
 - [47] D. Van Der Spoel, E. Lindahl, B. Hess, G. Groenhof, A. E. Mark, H. J. C. Berendsen, GROMACS: Fast, flexible, and free, *J. Comput. Chem.* 26 (2005) 1701–1718.
 - [48] M. J. Abraham, T. Murtola, R. Schulz, S. Páll, J. C. Smith, B. Hess, E. Lindahl, GROMACS: High performance molecular simulations through multi-level parallelism from laptops to supercomputers, *SoftwareX* 1-2 (2015) 19–25.
 - [49] H. Berendsen, D. van der Spoel, R. van Drunen, GROMACS: A message-passing parallel molecular dynamics implementation, *Comput. Phys. Commun.* 91 (1995) 43–56.
 - [50] S. O. Yesylevskyy, L. V. Schäfer, D. Sengupta, S. J. Marrink, Polarizable water model for the coarse-grained martini force field, *PLOS Computational Biology* 6 (2010) 1–17.
 - [51] T. A. Wassenaar, H. I. Ingólfsson, R. A. Böckmann, D. P. Tieleman, S. J. Marrink, Computational Lipidomics with insane : A Versatile Tool for Generating Custom Membranes for Molecular Simulations, *J. Chem. Theory Comput.* 11 (2015) 2144–2155.
 - [52] R. Hockney, S. Goel, J. Eastwood, Quiet high-resolution computer models of a plasma, *J. Comput. Phys.* 14 (1974) 148–158.
 - [53] L. Verlet, Computer “Experiments” on Classical Fluids. I. Thermodynamical Properties of Lennard-Jones Molecules, *Phys. Rev.* 159 (1967) 98–103.
 - [54] J. Dilger, S. McLaughlin, T. McIntosh, S. Simon, The dielec-

tric constant of phospholipid bilayers and the permeability of membranes to ions, *Science* 206 (1979) 1196–1198.

- [55] G. Gramse, A. Dols-Perez, M. A. Edwards, L. Fumagalli, G. Gomila, Nanoscale measurement of the dielectric constant of supported lipid bilayers in aqueous solutions with electrostatic force microscopy, *Biophys. J.* 104 (2013) 1257–1262.
- [56] H. J. C. Berendsen, J. P. M. Postma, W. F. van Gunsteren, A. DiNola, J. R. Haak, Molecular dynamics with coupling to an external bath, *J. Chem. Phys.* 81 (1984) 3684–3690.
- [57] G. Bussi, D. Donadio, M. Parrinello, Canonical sampling through velocity rescaling, *J Chem Phys.* 126 (2007) 014101.
- [58] M. Parrinello, A. Rahman, Polymorphic transitions in single crystals: A new molecular dynamics method, *J. Appl. Phys.* 52 (1981) 7182–7190.
- [59] C. Caleman, D. Van Der Spoel, Picosecond melting of ice by an infrared laser pulse: A simulation study, *Angew. Chem. Int. Ed.* 47 (2008) 1417–1420.
- [60] W. Humphrey, A. Dalke, K. Schulten, Vmd: visual molecular dynamics, *J. Mol. Graphics* 14 (1996) 33–38.
- [61] M. A. Heald, J. B. Marion, Classical electromagnetic radiation, Saunders College Pub., 1995. Using relative dielectric constant value of 14 from our model.
- [62] C. J. Pipe, G. H. McKinley, Microfluidic rheometry, *Mech. Res. Commun.* 36 (2009) 110–120.
- [63] F. Al-Niaimi, N. Y. Z. Chiang, Topical vitamin c and the skin: mechanisms of action and clinical applications, *J Clin Aesthet Dermatol* 10 (2017) 14.
- [64] E. Kechichian, K. Ezzedine, Vitamin d and the skin: an update for dermatologists, *Am J Clin Dermatol* 19 (2018) 223–235.
- [65] J. Brescoll, S. Daveluy, A review of vitamin b12 in dermatology, *Am J Clin Dermatol* 16 (2015) 27–33.
- [66] Y. Saray, A. T. Güleç, Treatment of keloids and hypertrophic scars with dermojet injections of bleomycin: a preliminary study, *Int J Dermatol* 44 (2005) 777–784.
- [67] S. Arbache, D. Roth, D. Steiner, J. Breunig, N. S. Michalany, S. T. Arbache, L. G. de Souza, S. H. Hirata, Activation of melanocytes in idiopathic guttate hypomelanosis after 5-fluorouracil infusion using a tattoo machine: Preliminary analysis of a randomized, split-body, single blinded, placebo controlled clinical trial, *J Am Acad Dermatol* 78 (2018) 212–215.